International Journal of Natural and Engineering Sciences
E-ISSN: 2146-0086 17(3): 110-120, 2023
Research Article

Microwave assisted solution combustion synthesis of ZnO nanoparticles: Effect of different urea concentrations and their photocatalytic investigations

L.N.Shubha[1]*, E.D.Sherly[2] Vaishnavi Kalode[3]

[1] *Department of Electronics , St. Francis College for Women, Begumpet, Hyderabad, India.*
[2] *Department of Chemistry , St. Francis College for Women, Begumpet, Hyderabad, India.*
[3] *Department of Chemistry , St. Francis College for Women, Begumpet, Hyderabad, India.*

*Corresponding author: shubhastfrancis@gmail.com

(Received: October 12, 2023 / Accepted: November 23, 2023)

Abstract

Zinc oxide nano particles (nano ZnO) is a fascinating photocatalyst due to its ability to absorb light in the Ultraviolet and Visible region. In the present study, by employing the microwave assisted solution combustion synthesis, 7 samples of nano ZnO (ZnO A - G) were synthesized by varying the fuel (urea) concentration. Zinc nitrate hexahydrate ($Zn(NO_3)_2.6H_2O$ was used as the metal precursor. As-synthesized Nano ZnO samples were characterized by powder X-ray diffraction (XRD), UV absorbance study, Fourier transform infra-red (FT-IR) spectroscopy and Field emission scanning electron spectroscopy (FE-SEM). Photocatalytic degradation (PCD) efficiency of ZnO samples was investigated by the degradation of methyl orange under UV light (365 nm) irradiation. It was found that ZnO synthesized with higher concentrations of urea (ZnO F and G) exhibited good PCD efficiency compared to ZnO A-E synthesized with lesser Urea concentrations.

Keywords: Nano ZnO, combustion synthesis, urea, photocatalytic degradation , PCD efficiency

Introduction

Researchers are encouraged to adopt innovative strategies and sustainable green initiatives to meet the growing demands of industrialization. Most of the technologies are focussed on reducing the waste and avoiding processes that are harmful to the environment. The combination of green chemistry based nanotechnological research has played a significant role in this direction. Particle size plays an important role in Nanotechnology. Nanoparticles show unusual characteristics than the larger particles of the same bulk substance due to greater surface area to volume ratio [1, 2]. Nano ZnO is one of the potential nano metal oxides. It is a n-type semiconductor with a wide band gap of 3.2 eV suitable for UV transitions [3] and shows very large exciton binding energy of 60 meV at room temperature, which leads to excitonic transitions [4]. Nano ZnO has distinctive electronic [5], piezoelectric [6], pyroelectric [7], physical [8] and biomedical properties [9]. The morphology and shape of ZnO NPs varies according to preparation techniques [10]. Due to its photo stability, it acts as an eminent photocatalyst used to photodegrade several organic pollutants. This property of ZnO NPs is used for water purification and disinfection treatment [11, 12].Commonly used synthetic methods for nano ZnO are simple precipitation [13], solvo thermal [14], wet chemical [15] and micro emulsion [16]. Solution Combustion Synthesis is an efficient synthetic method for nano ZnO. Here the stoichiometric redox reaction between the oxidiser and the fuel, which on attaining the ignition temperature, generates excess heat which self-propagates the reaction and undergoes auto-combustion [17]. The ash obtained is the desired nanoparticle. The exothermicity increases the temperature of the reaction >1000˚C. This method is also called Fire Synthesis as flame is lit during the reaction [18]. Oxidizer is the electron-acceptor for e.g., Metal Nitrate and Fuel is electron donor e.g., $-NH_2$ and -COOH containing hydrocarbons like Urea, Glycine and Citric acid. It provides C and H for CO_2, H_2O formation and heat liberation [19]. Combustion Synthesis when carried out in Microwave oven is termed as microwave assisted combustion synthesis (MACS) [20, 21]. This methodology is green, fast and the heat is distributed homogeneously over the content. Dipoles mobilize themselves with the oscillating microwave current. The back-and-forth movement of the molecules cause greater collision with each other and the walls of the container. Collisions generate tremendous amount of heat which raises the temperature and stimulates the reaction. In conventional heating, heat is supplied from outside to inside. In Microwave heating, heat is

generated by greater number of collisions and distributed homogeneously to the entire volume. Combustion Synthesis is instantaneous and sometimes improper heat control may turn the reaction explosive; such risks can be overcome by using microwave heating. Moreover, the microwave is placed in a fume hood such that the gases evolved do not pollute the lab environment. Comparative studies of different fuels such as urea, glycine and citric acid in Solution Combustion Synthesis (SCS) of nano ZnO have been reported [22].In the current work, we have prepared 7 samples of nano ZnO (A-G) by varying the concentration of urea (fuel) via microwave assisted solution combustion synthesis. The prepared ZnO samples were characterized by powder X-ray diffraction (XRD), UV-visible absorbance spectroscopy, Infrared spectroscopy (IR) and Field emission scanning electron microscopy (FESEM). Photocatalytic degradation (PCD) efficiency of the prepared ZnO samples was examined by the degradation of methyl orange solution.

Materials and Methods

Synthesis of nano ZnO

All the reagents used were of analytical grade. Zinc nitrate hexahydrate ($Zn(NO_3)_2.6H_2O$) was obtained from Hi Media, urea from Merck and methyl orange from SD Fine Chem Limited.

S.R. Jain et al. has reported that the stoichiometric compositions of the solution components (fuels and oxidizer) can be calculated according to the principle of propellant chemistry, keeping the oxidizer (metal nitrate) to fuel (urea) ratio as unity [23].

Oxidizing valency of $Zn(NO_3)_2$: 1(Zn) = +2 , 2(N) = 0 , 6 (O) = -12 ,
Total = +2-12 = -10

Reducing valency of CH_4N_2O: 1(C)= +4 , 4(H) = +4 , 1(O) = -2 , 2(N) = 0
Total = +4+4-2 = +6

$$\varphi e = \frac{(Total\ composition\ of\ oxidizing\ elements)}{(Total\ Composition\ of\ reducing\ elements)} = 10/6 = 1.67 \text{ [24]}$$

Therefore one mole of $Zn(NO_3)_2.6H_2O$ would require 1.67 moles of urea. 1M $Zn(NO_3)_2.6H_2O$ solution is prepared by dissolving 2.975 g $Zn(NO_3)_2.6H_2O$ in 10 ml distilled water and 1.67 M urea solution is prepared by dissolving 1.003 g in 10 ml distilled water. $Zn(NO_3)_2.6H_2O$ and urea (CH_4N_2O) solutions were mixed and stirred for 1 h to obtain a clear solution. This was placed in a domestic microwave-oven (2.45 GHz and 850 W) in a silica crucible for 7 minutes. Initially, the solution boiled and underwent dehydration followed by decomposition with the evolution of gases. When the solution reached the point of spontaneous combustion, it vaporized and instantly became a solid. The obtained solid was washed well with distilled water and ethanol and dried in a hot air oven at 80°C for 2 h. During combustion, the gaseous products released were N_2, NO_2, CO_2 and H_2O as water vapor.

We undertook the current study to see the effects of urea (fuel) concentration in the synthesis of nano ZnO. We kept the $Zn(NO_3)_2.6H_2O$ concentration to one mole while changing the urea concentrations. Best results are obtained with Zinc nitrate to urea ratio as 1: 3.3 and 1:4. The hygroscopic nature of zinc nitrate could be the reason for the requirement of more urea.

In all the 7 experiments, irrespective of the amount of urea used, there was combustion with flame at around 3 minutes into microwave heating and the solid that remained after the combustion is the ZnO nanoparticles. The pinkish coloration of the Samples 'A - G' is due to the excessive oxygen defects [25]. Samples 'F' and 'G' synthesized with more urea, was light pink colored porous solid NPs as shown in Figure 1. This can be based on porosity control principle. More the fuel, more the CO_2 liberated and higher the exothermic pressure which gave the NPs a fluffy texture. High Porosity causes high surface area which makes Sample 'F' and 'G' better photocatalysts [26].

Table 1. *$Zn(NO_3)_2.6H_2O$ concentration with varying concentration of urea*

Sample	**$Zn(NO_3)_2.6H_2O$ to urea molar ratio**	**Wt. of Urea**
A	1:1.67	1.0030 g
B	1:1.50	0.9027 g
C	1:1.83	1.1033 g
D	1:2	1.2036 g
E	1:2.67	1.6048 g
F	1:3.34	2.0060 g
G	1:4	2.4072 g

Figure 1. *Pink colour formation of ZnO samples with increase in Urea*

Characterization

The surface morphology analysis was performed by a field-emission scanning electron microscopy (FEI, Apreo S LoVac), at Central Analytical Laboratory, Birla Institute of Technology and Science, Hyderabad. The structures of the samples were investigated via Bruker X-ray diffractometer with Cu Kα radiation at λ = 1.540 Å at department of Chemistry, Osmania University, Hyderabad. The absorption spectra of the samples were recorded using UV-Visible spectrophotometer (Systronics) at St.Francis College for Women, Hyderabad. The FT-IR spectra were recorded on FT-IR spectrophotometer (Bruker Tensor 27) at department of Chemistry, Osmania University, Hyderabad.

Photocatalytic reactor set-up and degradation procedure

Photocatalytic degradation (PCD) experiments were carried out in a self-designed multi-lamp photocatalytic reactor (Heber Scientific) at St.Francis College for Women, Hyderabad as shown in Fig. 2 for UV light (365 nm) irradiation. The lamp housing consists of low-pressure mercury lamps (8×8W) emitting 365 nm light. Cylindrical borosilicate photocatalytic reactor tubes with a dimension of 36-1.6 cm (height-diameter) were

used. Methyl orange solution was prepared by dissolving 10 mg of methyl orange in 1000 ml of distilled water.

50 mg of synthesized ZnO sample was added to methyl orange solution (100 ml) and stirred for 30 minutes to reach the adsorption/desorption equilibrium and then transferred to the reactor tube. This was placed inside the reactor setup and subjected to irradiation. Air was continuously bubbled into the reactor tube by an air pump during irradiation and the contents in the reactor tubes was stirred magnetically with the help of a rice pellet magnetic bead.

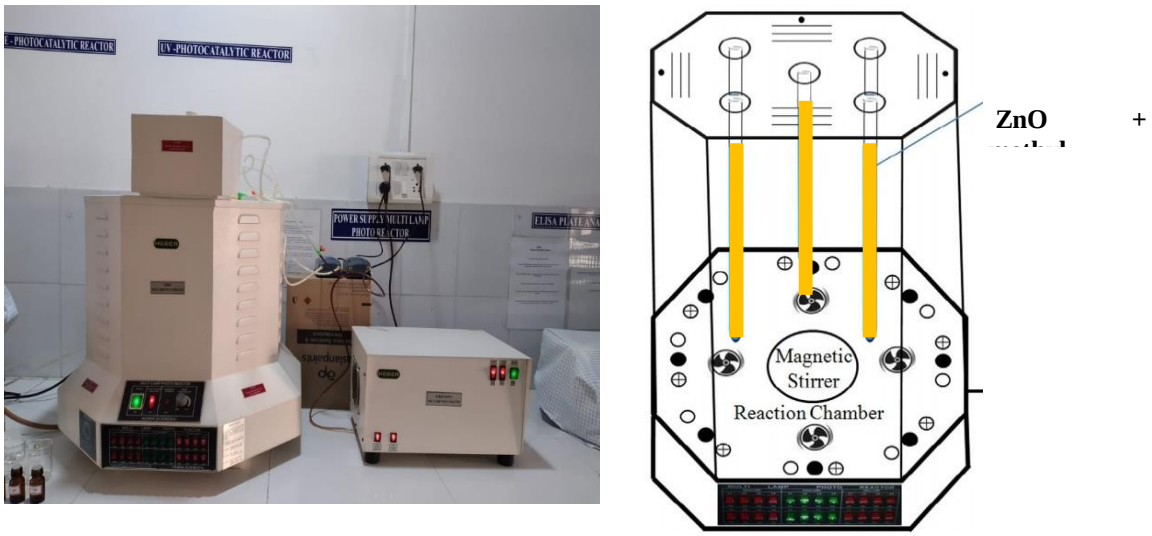

Figure 2. *UV-Photocatalytic reactor*

Results and Discussion

X-ray diffraction analysis

X-ray diffraction pattern of ZnO Samples is shown in **Fig. 3**. All the samples gave sharp diffraction peaks indicating the crystallinity of the samples. The diffraction peaks are observed at 2θ = 31.5633, 34.2385, 36.0198, 47.3645, 56.3871, 62.6925, 66.2090, 67.7587, 68.8746 with [100], [002], [101], [102], [110], [103], [200], [112] and [201] planes respectively which matches with the hexagonal wurtzite morphology of ZnO [27,28]. The same XRD patterns of all the samples indicate that ZnO hexagonal wurtzite structure is conserved in all the ZnO NP samples. This implies that there is no effect of urea (fuel) on crystallinity. As the diffractogram has no other peaks other than ZnO, it denotes that all the samples contain only ZnO NPs and no other impurities.

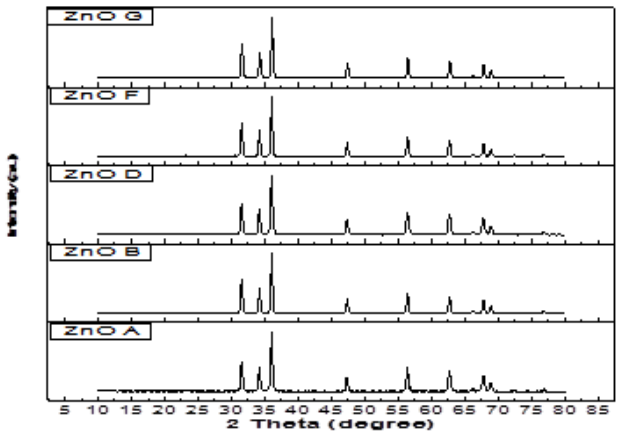

Figure 3. *XRD pattern of ZnO Samples A,B,D,F and G*

The ZnO crystallite size can be calculated by utilizing the Debye – Scherrrer formula [4].

$$d = \frac{0.89\lambda}{\beta \cos\theta}$$

Where d = Crystal size

0.89 = Scherrer's constant

β = FWHM (Full Width at Half Maximum)

ʎ = Wavelength of X-rays = 1.540 A˚

θ = Bragg's Diffraction Angle

Crystallite sizes of samples A, B, D, F and G are given in Table 2.

Table 2. *Crystallite size determination*

K = 0.89 ; ʎ = 0.154 nm ; 1 degree = 0.017453 radian

Sample	2 Theta (degree)	Theta (degree)	Theta (Radian)	Cos θ (Radian)	FWHM (degree)	FWHM (Radian)	Crystallite Size (nm)
A	36.0198	18.0099	0.314330	0.999984	0.3936	0.00686	19.9516
B	36.0475	18.0237	0.314573	0.999984	0.4723	0.00824	16.6273
D	36.0201	18.0101	0.314334	0.999984	0.3936	0.00686	19.9519
F	36.0475	18.0237	0.314573	0.999984	0.4723	0.00824	16.6273
G	36.0934	18.0467	0.314974	0.950804	0.3936	0.00686	20.9839

FT-IR analysis

The FTIR spectra of ZnO samples A, B, D, F and G are shown in **Fig. 4**. IR Spectra are recorded in the region of 400-4000 cm^{-1}. All the samples showed a peak around 360-438 cm^{-1} attributed to the characteristic absorption band of the Zn-O bond . Peak at 2352 - 2358 cm^{-1} is due to C- O stretching of CO_2 and O-H stretching peak is at 3427 - 3451 cm^{-1} [29,30].

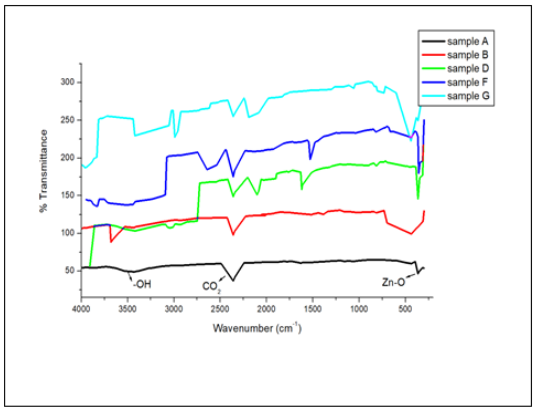

Figure 4. *IR Spectra of ZnO Samples A,B,D,F and G*

Absorbance spectra of ZnO

Absorption spectra of ZnO samples were recorded after dispersing the ZnO in ethanol by sonication. The UV-Vis absorption spectra of Samples A through G are shown in **Fig. 5**. Samples F and G also displayed a significant UV absorbance peak at 379 nm. All of the samples displayed a robust excitonic absorption peak around 257 nm [4]. ZnO samples F and G could absorb the UV radiation of 365 nm and act as an efficient photocatalyst because the photocatalytic degradation studies were conducted at this wavelength.

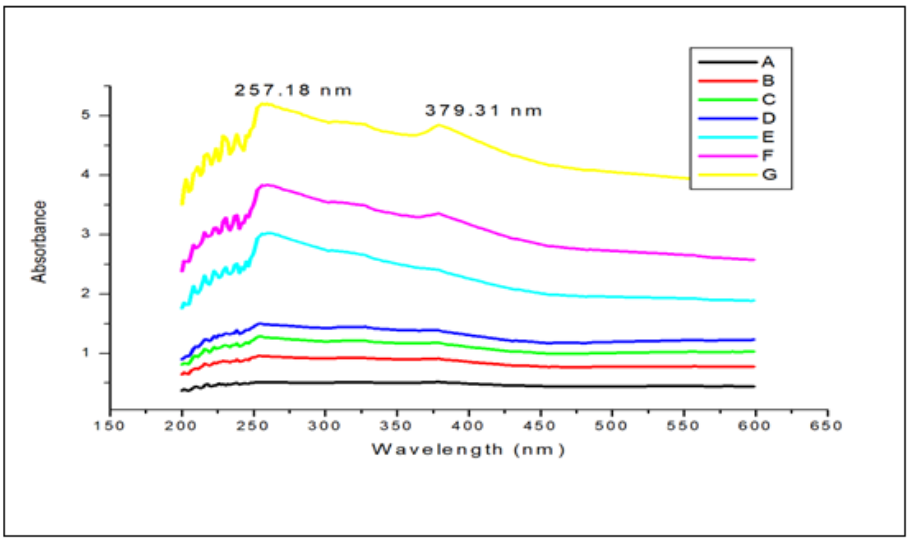

Figure 5. *Absorbance Spectra of ZnO samples A- G*

FESEM analysis

Morphology of the synthesized ZnO NPs was studied using FESEM. In SCS, tremendous amount of heat energy is expelled due to which control over the growth of the synthesized NPs cannot happen, hence we have obtained nanoparticle aggregates [3]. Fig. 6 (a) and (b) are the FESEM images of ZnO-A and and (c) and (d) are of ZnO-F.

ZnO-A has nano triangles cluster morphology whereas ZnO-F has spherical morphology. The high concentration of urea has changed the morphology of Nano ZnO. Nanotriangle structure of ZnO-A and Nanospheres for ZnO-F are clearly seen in Figures (b) and (d) respectively. Spherical ZnO-F sample has highly porous surface and small particle size compared to ZnO-A.

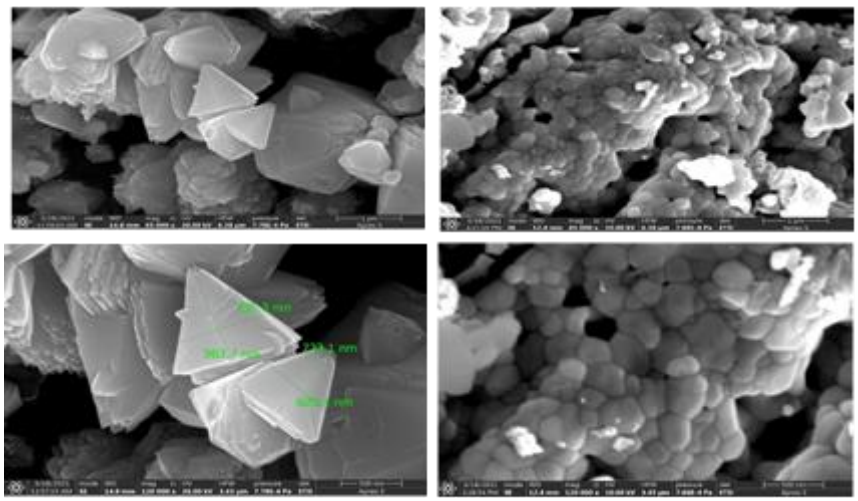

Figure 6. *FESEM images of ZnO-A (a,b) and ZnO-F (c,d)*

Photocatalytic degradation study of methyl orange using ZnO as photocatalyst

ZnO NPs have band gap of 3.2 eV which is suitable for absorbing UV light. Since ZnO is a photocatalytst, it gets excited on irradiation with UV light. Electron/hole pairs are generated; most of them will recombine by emitting heat. But some of these electron/hole pairs can generate highly reactive hydroxyl radicals which in turn can degrade methyl orange.

The photodegradation was carried out for 3.5 h. After every half an hour, the setup was paused and 5ml of methyl orange solution was withdrawn in dark brown bottles. Methyl orange solution turned colorless after 3.5 h of photodegradation on ZnO-F and ZnO-G. Fig. 7 a and b represents the photographs of photodegradation before and after 3.5 hours respectively.

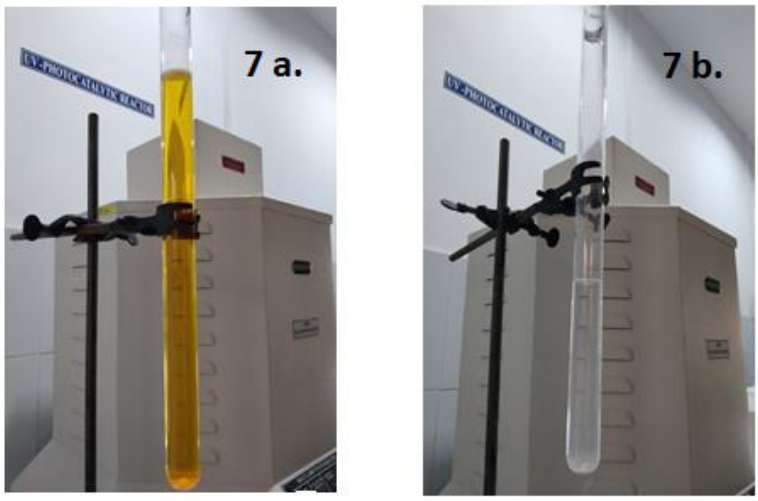

Figure 7 a and b *represents the photographs of photodegradation before and after 3.5 hours*

The extent of methyl orange degradation was monitored by using UV–Visible spectrophotometer. The absorbance was measured for the samples withdrawn from the reaction tubes every 30 min time intervals in the wavelength range of 200 to 600 nm. Graph was plotted with absorbance value on the y axis and wave length on the x axis. PCD Efficiency was calculated by using the equation,

where, $\mathbf{A_0}$= Initial absorbance of methyl orange before photodegradation $\mathbf{A_t}$=Absorbance of methyl orange after time 't'.

ZnO samples A-E did not give effective photodegradation of methyl orange solution. Whereas ZnO-F and ZnO-G prepared with more urea gave efficient degradation as shown in Fig. 8 a, b and c.

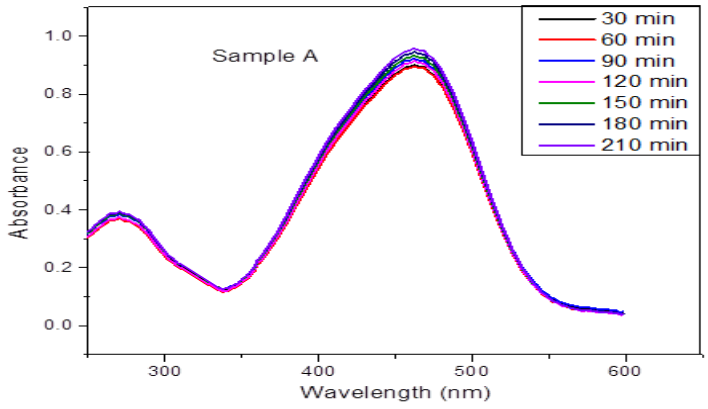

Fig. 8 a. Photocatalytic degradation on ZnO-A

$$\eta = \frac{A_0 - A_t}{A_0} \times 100$$

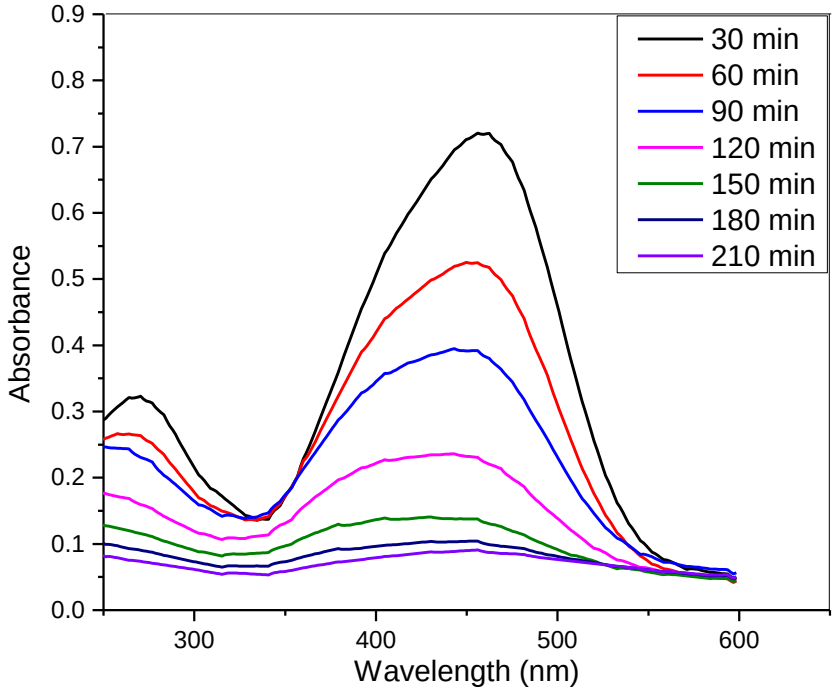

Time (t)	Absorbance
0 min	0.887
30min	0.714
60min	0.511
90min	0.375
120min	0.219
150min	0.130
180min	0.099
210min	0.087

Figure 8 b. *Photocatalytic degradation on ZnO-F*

$A_o = 0.887$; $A_t = 0.087$

$$\eta = \frac{A_0 - A_t}{A_0} \times 100$$

$$\eta = \frac{0.887 - 0.087}{0.887} \times 100$$

$$\eta = \frac{0.8}{0.887} \times 100 = 90.19$$

n = 90.19 %

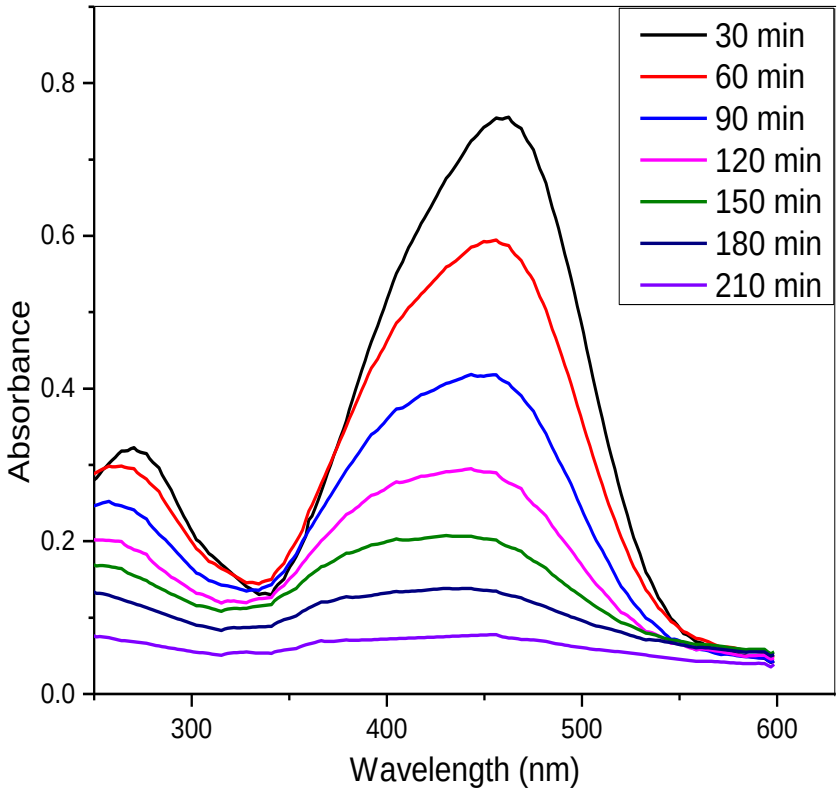

Time (t)	A_t of MO
0min	0.887
30min	0.749
60min	0.5806
90min	0.402
120min	0.275
150min	0.191
180min	0.129
210min	0.073

Figure 8 c. *Photocatalytic degradation on ZnO-G*

$$\eta = \frac{A_0 - A_t}{A_0} \times 100$$

$$\eta = \frac{0.887 - 0.073}{0.887} \times 100$$

$$\eta = \frac{0 \cdot 814}{0 \cdot 887} \times 100 = 91.77$$

η = 91.77% %

ZnO-F and ZnO-G was able to attain 90.19 % and 91.77% of photocatalytic degradation of methyl orange respectively. The absorbance spectra of the ZnO samples as shown in Figure 5, revealed that only samples F and G had a strong absorbance peak around 390 nm. As the photocatalytic degradation was carried out at 365 nm, ZnO-F and G was able to absorb in this region while the other ZnO samples could not absorb the UV radiation. Larger surface area due to the small particle size and porosity of samples F and G are other factors which contributed to the efficient photocatalytic degradation of methyl orange on these samples.

Conclusions

In order to examine the effect of Urea (Fuel) concentration on Microwave assisted solution combustion synthesis, 7 different nano ZnO samples were prepared by varying urea concentration while keeping the zinc nitrate concentration constant. Nano ZnO Samples A - E synthesized with lesser urea had a pinkish tint and powdery texture whereas the nano ZnO samples F and G synthesized with more urea had light pink coloration, disintegrated and porous texture. On examining the FE-SEM images of sample A and F revealed that on increasing the urea concentration, the morphology changed to uniform spherical shape with large pores and much smaller particle size for ZnO F. The absorbance study of the ZnO samples showed that only samples F and G had a strong absorbance peak at 379 nm, which would facilitate excitation on irradiation

with 365 nm UV light. ZnO-F and G exhibited efficient photocatalytic degradation of methyl orange on irradiation with 365 nm light while other samples showed minimum degradation under the same experimental conditions. Increasing the urea (fuel) concentration has reduced the particle size and improved the porosity of the ZnO samples and this has tremendously improved PCD efficiency.

References

[1] Baig, N., Kammakakam, I., & Falath, W. (2021). Nanomaterials: A review of synthesis methods, properties, recent progress, and challenges. *Materials Advances*, *2*(6), 1821-1871.

[2] Khan, I., Saeed, K., & Khan, I. (2019). Review nanoparticles: properties, applications and toxicities. *Arab J Chem*, *12*(2), 908-931

[3] Sherly, E. D., Vijaya, J. J., Selvam, N. C. S., & Kennedy, L. J. (2014). Microwave assisted combustion synthesis of coupled ZnO–ZrO2 nanoparticles and their role in the photocatalytic degradation of 2, 4-dichlorophenol. *Ceramics International*, *40*(4), 5681-5691.

[4] Talam, S., Karumuri, S. R., & Gunnam, N. (2012). Synthesis, characterization, and spectroscopic properties of ZnO nanoparticles. *International Scholarly Research Notices*, *2012*.

[5] Singh, A. K. (2010). Synthesis, characterization, electrical and sensing properties of ZnO nanoparticles. *Advanced Powder Technology*, *21*(6), 609-613.

[6] Li, G. Y., Zhang, H. D., Guo, K., Ma, X. S., & Long, Y. Z. (2020). Fabrication and piezoelectric-pyroelectric properties of electrospun PVDF/ZnO composite fibers. *Materials Research Express*, *7*(9), 095502.

[7] Panwar, V., Nandi, S., Majumder, M., & Misra, A. (2022). Self-powered ZnO based pyro-phototronic photodetectors: Impact of heterointerfaces and parametric studies. *Journal of Materials Chemistry C*.

[8] Lv, J., Li, C., & Chai, Z. (2019). Defect luminescence and its mediated physical properties in ZnO. *Journal of Luminescence*, *208*, 225-237.

[9] Karthick, R., Sakthivel, P., Selvaraju, C., & Paulraj, M. S. (2021). Tuning of photoluminescence and antibacterial properties of ZnO nanoparticles through Sr doping for biomedical applications. *Journal of Nanomaterials*, *2021*, 1-7.

[10] Zaouk, D., Zaatar, Y., Asmar, R., & Jabbour, J. (2006). Piezoelectric zinc oxide by electrostatic spray pyrolysis. *Microelectronics journal*, *37*(11), 1276-1279.

[11] Jiang, J., Pi, J., & Cai, J. (2018). The advancing of zinc oxide nanoparticles for biomedical applications. *Bioinorganic chemistry and applications*, *2018*.

[12] Sadeghi, B. (2014). Preparation of ZnO/Ag nanocomposite and coating on polymers for anti-infection biomaterial application. *Spectrochimica Acta Part A: Molecular and Biomolecular Spectroscopy*, *118*, 787-792.

[13] Sadeghi, B. (2018). Synthesis and characterization of ultrafine Ag/ZnO nanotetrapods (AZNTP) for environment humidity sensing. *Avicenna Journal of Environmental Health Engineering*, *5*(2), 115-119.

[14] Sadeghi, B. (2018). Controlled growth and characterization Ag/ZnO nanotetrapods for humidity sensing. *Combinatorial Chemistry & High Throughput Screening*, *21*(7), 462-467.

[15] Chen, C. C., Fan, H. J., & Jan, J. L. (2008). Degradation pathways and efficiencies of acid blue 1 by photocatalytic reaction with ZnO nanopowder. *The Journal of Physical Chemistry C*, *112*(31), 11962-11972.

[16] An, L. J., Wang, J., Zhang, T. F., Yang, H. L., & Sun, Z. H. (2012). Synthesis of ZnO nanoparticles by direct precipitation method. In *Advanced Materials Research* (Vol. 380, pp. 335-338). Trans Tech Publications Ltd.

[17] Ghoshal, T., Biswas, S., Paul, M., & De, S. K. (2009). Synthesis of ZnO nanoparticles by solvothermal method and their ammonia sensing properties. *Journal of Nanoscience and Nanotechnology*, *9*(10), 5973-5980.

[18] Shimpi, N. G., Jain, S., Karmakar, N., Shah, A., Kothari, D. C., & Mishra, S. (2016). Synthesis of ZnO nanopencils using wet chemical method and its investigation as LPG sensor. *Applied Surface Science*, *390*, 17-24.

[19] Wang, Y., Zhang, X., Wang, A., Li, X., Wang, G., & Zhao, L. (2014). Synthesis of ZnO nanoparticles from microemulsions in a flow type microreactor. *Chemical Engineering Journal*, *235*, 191-197.

[20] Mimani, T. (2000). Fire synthesis: Preparation of alumina products. *Resonance*, *5*(2), 50-57.

[21] Głowniak, S., Szczęśniak, B., Choma, J., & Jaroniec, M. (2021). Advances in microwave synthesis of nanoporous materials. *Advanced Materials*, *33*(48), 2103477.

[22] Patil, K. C., Aruna, S. T., & Ekambaram, S. (1997). Combustion synthesis. *Current opinion in solid state and materials science*, *2*(2), 158-165.

[23] Köseoğlu, Y. (2014). A simple microwave-assisted combustion synthesis and structural, optical and magnetic characterization of ZnO nanoplatelets. *Ceramics International*, *40*(3), 4673-4679.

[24] Lucilha, A. C., Afonso, R., Silva, P. R., Lepre, L. F., Ando, R. A., & Dall'Antonia, L. H. (2014). ZnO prepared by solution combustion synthesis: characterization and application as photoanode. *Journal of the Brazilian Chemical Society*, *25*, 1091-1100.

[25] Jain, S. R., Adiga, K. C., & Verneker, V. P. (1981). A new approach to thermochemical calculations of condensed fuel-oxidizer mixtures. *Combustion and flame*, *40*, 71-79.

[26] Husairi, F. S., Ali, S. M., Azlinda, A., Rusop, M., & Abdullah, S. (2013). Special effect of urea as a stabilizer in thermal immersion method to synthesis porous zinc oxide nanostructures. *Journal of Nanomaterials*, *2013*, 148-148.

[27] Cullity, B. D., & Stock, S. R. (2014). Elements of X-ray diffraction 3rd ed.

[28] Zak, A. K., Abrishami, M. E., & Abd, W. H. (2011). Majid, Ramin Yousefi, SM Hosseini. *Ceram Int*, *37*, 393-398.

[29] Shamhari, N. M., Wee, B. S., Chin, S. F., & Kok, K. Y. (2018). Synthesis and characterization of zinc oxide nanoparticles with small particle size distribution. *Acta Chimica Slovenica*, *65*(3), 578-585.

[30] Chitradevi, T., Jestin Lenus, A., & Victor Jaya, N. (2020). Structure, morphology and luminescence properties of sol-gel method synthesized pure and Ag-doped ZnO nanoparticles. *Materials Research Express*, *7*(1), 015011.